Large-Scale Ionospheric Modifications Produced by Nonlinear Refraction of an hf Wave

J. D. Hansen, G. J. Morales, L. M. Duncan,[a] J. E. Maggs, and G. Dimonte[b]
Physics Department, University of California, Los Angeles, California 90024-1547
(Received 24 May 1990)

We report experimental observations and computer modeling results of large-scale density and temperature modifications (several km extent, $\delta T_e/T_{e0}\sim 3$, $|\delta n_e|/n_{e0}\sim 25\%$) created in a low-density, midlatitude, night-time ionosphere by nonlinear refraction of an hf beam launched from a ground-based antenna. The process consists of the reorientation of the reflection surface parallel to the geomagnetic field lines and results in intense heating.

PACS numbers: 52.35.Mw, 52.40.Db, 94.20.Bb, 94.20.Vv

Large-scale density modifications can be produced in the ionosphere by localized temperature perturbations generated by a powerful hf wave (total power $\sim$400 kW, effective radiated power $\sim$100 MW) near its reflection layer. A schematic of the relevant experimental geometry is shown in Fig. 1. Large perturbations ($\delta T_e/T_{e0}\sim 3$, $|\delta n_e|/n_{e0}\sim 25\%$) caused by hf heating were first observed by Duncan, Sheerin, and Behnke[1] at the Arecibo Observatory in 1985 during solar minimum. Subsequent experiments (1986–1987) examined several features of these modifications including cavity dynamics in a high-neutral-wind environment,[2] but produced no quantitative conclusions regarding the mechanism responsible for their generation. In this Letter we report experimental observations of steady-state large perturbations obtained during 3–6 May 1988 and make quantitative comparisons with a two-dimensional transport model. It is found that reorientation of the wave reflection surface parallel to the geomagnetic field and subsequent heating confined to a narrow flux tube (i.e., nonlinear refraction) is the principal mechanism responsible for the generation of the large perturbations.

Experimental results from the heating campaign of 3–6 May 1988 at the Arecibo Observatory clearly indicate that large modifications evolve in time from a broad and symmetric heating profile (characteristic of the linear hf beam envelope) to narrow hot flux tubes shifted northward of the original heated region. The nonlinear evolution is observed to attain a highly reproducible universal asymptotic state. The principal diagnostic used is the received backscattered power of the 430-MHz radar at Arecibo as a function of altitude. The received backscattered power can be approximated[3] by

$$P=\frac{\alpha n_e}{1+T_e/T_i}, \tag{1}$$

with α a constant dependent on radar parameters, T_e/T_i the electron-ion temperature ratio, and n_e the electron density. Both density depletions and temperature increases simultaneously cause a decrease in the received signal strength. Figure 2 shows the backscattered signal of a typical asymptotic state achieved after 10–15 min of heating; for reference, the averaged unperturbed profile is also shown. The sharp decrease seen in Fig. 2 corresponds to simultaneous heating and density depletion along a narrow flux tube intersected at an angle of about 40° by the diagnostic radar, as illustrated in Fig. 1.

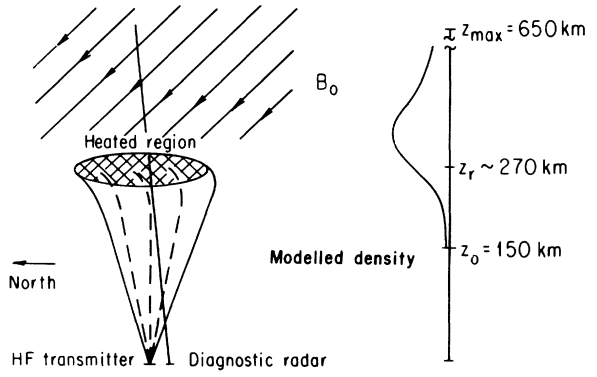

FIG. 1. Schematic of midlatitude ionospheric-modification experiment and night-time density profile.

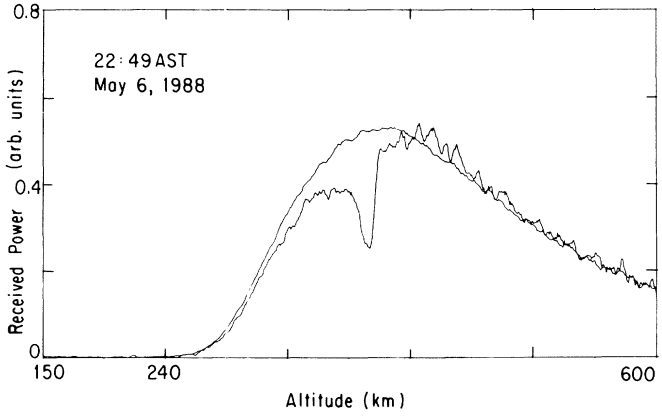

FIG. 2. Asymptotic steady state of large perturbation at 22:49 AST (AST denotes Atlantic Standard Time). The hf beam parameters are $f=4.45$ MHz, $P=400$ kW, on at 22:34 AST. The smooth curve is the averaged unperturbed profile.

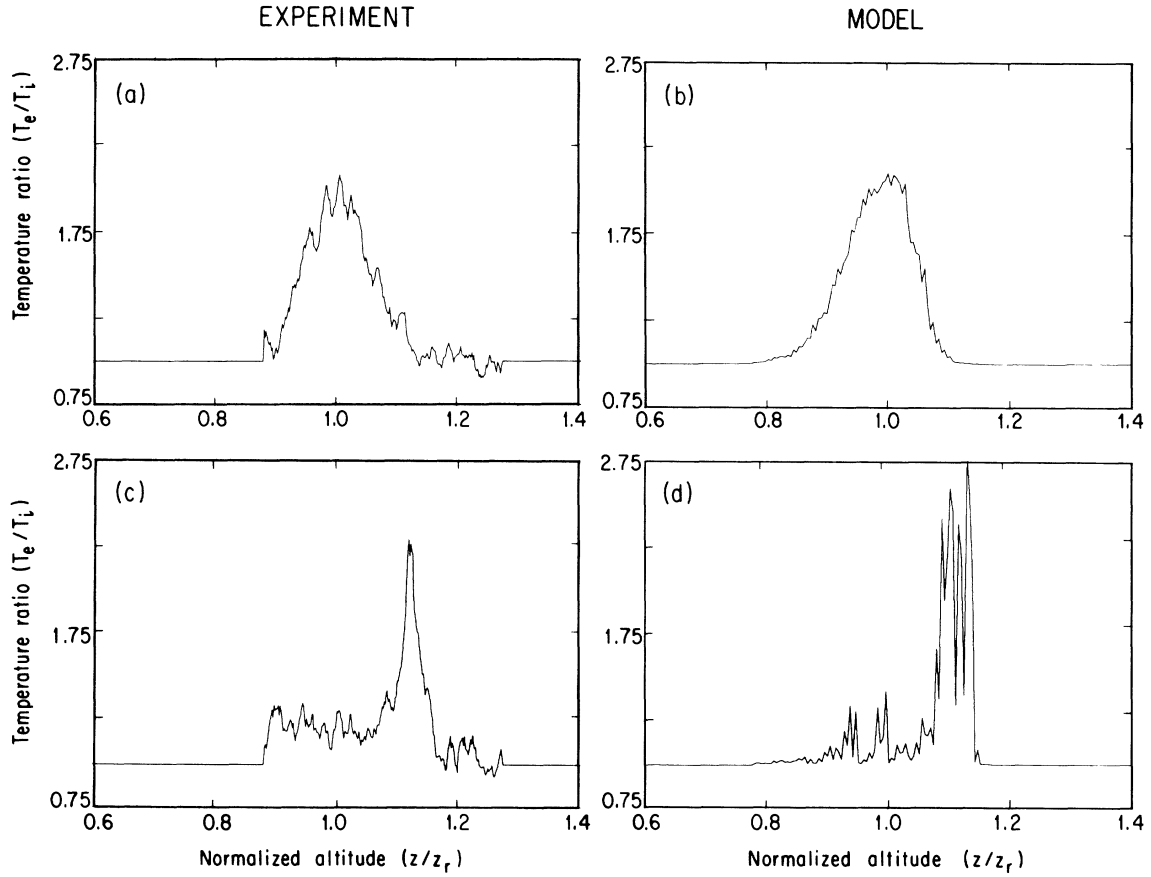

FIG. 3. Comparison of experimentally determined electron-ion temperature ratio of heated profiles with nonlinear refraction model for (a),(b) early stage and (c),(d) late stage as a function of normalized altitude (z/z_r). z_r is the reflection layer. The hf beam parameters are $f=4.45$ MHz, $P=400$ kW, on at 21:21:30 AST with $z_r\sim 357$ km. Model results are with $z_r=272$ km.

The experimentally determined two-stage time evolution of the temperature profile is displayed in Figs. 3(a) and 3(c) and is obtained from Eq. (1) as follows. In both early and late stages, the density dependence contained in Eq. (1) is removed by dividing the received backscatter signal by that obtained from a cold (i.e., $T_e/T_i=1$) reference profile having a similar density. For the early stage when density depletions are small, the reference profile used in the division is the unperturbed profile obtained just before the hf beam is turned on. For the late stage (i.e., the steady state), the reference profile used is obtained 2 min after the hf beam is turned off when the temperature ratio has fully relaxed to its original value ($T_e/T_i=1.0$), but the density has not relaxed appreciably. The horizontal axis of Figs. 3(a) and 3(c) is altitude normalized by the reflection height (obtained from plasma line data) of the hf wave ($z_r\sim 357$ km).

Figure 3(a) displays the experimentally determined change in temperature for the early stage of heating. With the aid of Fig. 1 it is easy to understand the geometrical relationship between the initially horizontal hf heating pattern, the oblique field lines along which heat transport occurs, and the vertically directed diagnostic radar. With this perspective, the symmetric Gaussian-like pattern shown in Fig. 3(a) can be simply interpreted as a mapping of the unperturbed hf beam pattern onto the diagnostic beam. In contrast, the late-time asymptotic stage shown in Fig. 3(c) exhibits a transition from this broad heating pattern to a narrow layer at an apparently higher altitude. Again referring to the geometry sketched in Fig. 1, this implies a simultaneous northward shift and horizontal shrinkage of the heated region.

Figure 3(c) indicates a nonlinear modification of the heating pattern. Our analysis demonstrates that this type of pattern results from nonlinear refraction caused by large heater-induced density depletions. To illustrate this point Fig. 4 shows O-mode ray trajectories[4] in a field-aligned density cavity of magnitude $|\delta n_e|/n_{e0}=0.3$ as could result from hf heating (reflected rays have been omitted for clarity). It is seen that the reflection surface ($\omega_{pe}=\omega_{\rm hf}$) is aligned with the geomagnetic field at some locations. In Fig. 4, the geomagnetic-field line labeled A

represents a flux tube on the northern edge of the perturbed region. Since most of the energy of the hf beam is absorbed near the O-mode reflection layer, the radiation propagates through the flux tube represented by the field line labeled B to create intense localized heating of the narrow flux tube at position A and simultaneous lowering of the heating that occurs at B in the absence of the density depletion.

For low-wind conditions the particle and heat transport occurs predominantly along the geomagnetic field, and the process can be described by the one-dimensional energy and continuity equations

$$\frac{3}{2}\left\{n_e\frac{\partial T_e}{\partial t}+n_e v_s\frac{\partial T_e}{\partial s}\right\}+n_e T_e\frac{\partial v_s}{\partial s}=\frac{\partial}{\partial s}\left[\kappa_e\frac{\partial T_e}{\partial s}\right]+Q-L_e\,, \tag{2}$$

$$\frac{\partial n_e}{\partial t}=\frac{\partial}{\partial s}\left\{D\left[\frac{\partial}{\partial s}[n_e(T_e+T_i)]+n_e m_i g\sin\theta\right]-n_e u\cos\theta\right\}-\beta n_e+S_i\,, \tag{3}$$

$$n_e v_s=-D\left[\frac{\partial}{\partial s}[n_e(T_e+T_i)]+n_e m_i g\sin\theta\right]+n_e u\cos\theta\,, \tag{4}$$

with s the coordinate along the magnetic field, v_s the field-aligned flow velocity, m_i the ion mass, u the neutral-wind velocity in the north-south direction, θ the magnetic-field dip angle, Q the hf source, S_i the local ionization source, and κ_e, L_e, D, and β the coefficients of thermal conduction, cooling, density diffusion, and recombination, respectively.[5,6] A transport code is used to solve these equations using a predictor-corrector tridiagonal method. Two-dimensional effects are modeled in the meridian plane by solving on many adjacent field lines.

To model nonlinear refraction effects, the absorption term Q in the transport code is modified as a function of time. Density and temperature perturbations due to the hf source are typically solved on 51 adjacent field lines spaced in the meridian plane by 2 km. The effect of the density changes on the spatial distribution of Q is computed as follows. At $t=0$ the unperturbed heat source Q consists of two Gaussian spatial dependences. One is in the horizontal direction and accounts for the hf beam footprint, having a typical width of 40 km. The other Gaussian describes the heat deposition along a given field line and is centered in altitude at the unperturbed reflection layer; it has a typical width of 5 km and represents the absorption that occurs near the main Airy lobe of the hf wave. As the density evolves, the modified reflection surface (the locus of the points $\omega_{pe}=\omega_{\rm hf}$) is calculated. The local value of Q at $t=0$ is used to weight ray trajectories that connect the unperturbed reflection surface with the modified one. As illustrated in Fig. 4, O-mode rays near reflection have group velocity nearly perpendicular to the magnetic field; thus the hf rays are extended across the field until they intercept the modified reflection surface at a point which generally lies between two field lines. The modified Q assigned to each field line is then obtained by summing over all projected rays that intersect the modified reflection surface between two field lines. This contribution is partitioned between the two adjacent field lines depending on the distance between the reflection point and the field line. This interpolation procedure is required because the contour of the modified reflection surface does not generally coincide with the grid points used in the calculation.

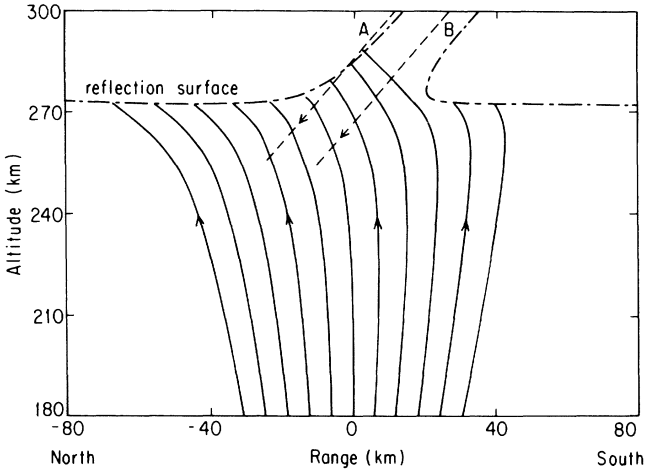

FIG. 4. Ray trajectories for an upward propagating O-mode beam in a prescribed field-aligned density cavity $|\delta n_e|/n_{e0}=0.3$. Labels A and B illustrate geomagnetic-field lines intersecting different regions of the beam.

Temperature values along a vertical line cutting across the field lines (see Fig. 1) are used to simulate the experimental radar diagnostic. The computational results are shown in Figs. 3(b) and 3(d). To avoid difficulties caused by the unknown boundary conditions at the high-altitude boundary, a lower altitude is chosen for the computer-model reflection layer ($z_r=272$ km) than is actually realized in the experiment ($z_r\sim 357$ km). However, a meaningful quantitative comparison of the hf heating effects can be obtained by normalizing the altitude scale of the profiles by the respective reflection heights. The parameters of the modeled hf beam (total power 400 kW, absorption efficiency $\sim 21\%$) are chosen to produce good agreement with the early stage (i.e., linear) experimental results. Similarities between exper-

iment [3(a)] and model [3(b)] include the magnitudes ($T_e/T_i \sim 2.0$) and the normalized widths at half maximum (0.14 and 0.13, respectively) of the perturbations. The late-stage results also show quantitative agreement in both magnitudes ($T_e/T_i \sim 2.3$ and 2.5) and normalized widths (0.051 and 0.055). The details of the fine structure obtained from the model in the late stage are an artifact of the discrete mesh of the code.

The close quantitative agreement found between the model results and experimental observations strongly suggests that nonlinear refraction is responsible for the generation of the observed large perturbations. Code results [similar to Figs. 3(b) and 3(d)] using the same hf power without inclusion of the nonlinear refraction model show no northward shift and remain Gaussian-like. Also, the model of the hf beam used in the code is detailed enough to produce quantitative agreement with the observations, yet by its simplicity, precludes different interpretations. The hf model simply assumes that the hf energy is absorbed in a region near the reflection surface. This makes the results independent of the specific mechanism (collisional or anomalous) of heat deposition. Also omitted is modeling of the self-focusing instability[7,8] which may occur coincident with the processes modeled in this paper, but on spatial scales significantly smaller (hundreds of meters compared to several kilometers) and in the underdense region of the plasma, provided Ohmic absorption is sufficiently large and local cooling and heat conduction are weak. However, the possible occurrence of self-focusing does not invalidate the phenomena described here. At the reflection layer, the dominant process is nonlinear refraction, i.e., the self-consistent reorientation of the reflection surface to a field-aligned geometry resulting in intense heating along a single narrow flux tube.

In conclusion, we have presented experimental and modeling results that demonstrate that large density and temperature perturbations can be produced in the ionosphere by hf waves. It should be stated that such results seem to depend upon ambient conditions most easily attained in low-density ionospheres during night-time conditions. We have shown that these results can be accurately modeled using a transport code and a simple hf model. These results demonstrate that the key process is nonlinear refraction of the hf beam across the geomagnetic field.

This work was supported by the Office of Naval Research and the Plasma Physics Research Institute at Lawrence Livermore National Laboratory under Contract No. B089352. Arecibo Observatory is operated by Cornell University under the sponsorship of the National Science Foundation.

[a]Permanent address: Clemson University, Clemson, SC 29634.

[b]Permanent address: Lawrence Livermore National Laboratory, Livermore, CA 94550.

[1]L. M. Duncan, J. P. Sheerin, and R. A. Behnke, Phys. Rev. Lett. **61**, 239 (1988).

[2]P. A. Bernhardt, L. M. Duncan, and C. A. Tepley, J. Geophys. Res. **94**, 7003 (1989).

[3]J. V. Evans, Proc. IEEE **57**, 496 (1969).

[4]R. M. Jones, Institute for Telecommincations, Sciences, and Aeronomy ESSA Technical Report No. IER-17/ITSA-17, 1968 (unpublished).

[5]M. M. Shourcri, G. J. Morales, and J. E. Maggs, J. Geophys. Res. **89**, 2907 (1984).

[6]J. D. Hansen, G. J. Morales, and J. E. Maggs, J. Geophys. Res. **94**, 6833 (1989).

[7]F. W. Perkins and E. J. Valeo, Phys. Rev. Lett. **32**, 1234 (1974).

[8]L. M. Duncan and R. A. Behnke, Phys. Rev. Lett. **41**, 998 (1978).